N79-20050

D20

20

IMPROVED PREDICTION OF LAMINAR LEADING EDGE SEPARATION

R. N. Herring and W. L. Ely
McDonnell Aircraft Company
McDonnell Douglas Corporation

SUMMARY

This research was conducted in order to provide a definite criterion for the prediction of the bubble burst on airfoils typical of those used for fighter wings. The approach taken was to correlate existing airfoil bubble burst data using various parameters at the laminar separation point. The method due to Weber was modified to provide a continuous analytic solution for the velocity distribution around the airfoil leading edge. This proved to be as accurate as any available. Coupling the modified Weber method with the Stratford laminar separation prediction method leads to a universal chart giving the conditions at separation as a function of stagnation location and leading edge radius. Application of the combined method to available two-dimensional airfoil data resulted in an empirical criterion presenting the limiting local velocity gradient at separation as a function of the boundary layer momentum thickness at separation for bubble burst. The correlation leads as well to the qualitative explanation of two types of laminar stall: thin airfoil and leading edge. The validity of the correlation is demonstrated by predicting the lift coefficient and angle of attack for stall on airfoils with leading edge or trailing edge flaps.

INTRODUCTION

Airfoil laminar bubble burst is the cause of excessive drag due to lift on very thin airfoils and of maximum lift stalling on moderately thin airfoils. It has been the subject of considerable experimental and theoretical research. However, efforts to apply previous research to the subject of maneuvering drag due to lift on swept thin wings typical of transonic fighter aircraft proved unrewarding. The present research was undertaken to provide the basis of a technique to predict laminar bubble burst on such wings.

As pointed out by Goradia and Lyman (Reference 1) bubble burst is quite likely to be a function of conditions at the laminar separation point. The problem therefore consists of determining those conditions and correlating the experimental data.

NOMENCLATURE

A	Average value of A(x)
A(x)	Velocity ratio due to thickness at $\alpha = 0$
B	Average value of B(x)

$B(x)$	Velocity ratio due to thickness at angle of attack
C_L	Lift coefficient
g	One half the leading edge radius divided by chord
R_c	Freestream Reynolds number based on chord
R_θ	Local Reynolds number based on momentum thickness
s	Arc length along the airfoil surface, divided by chord
u	The ratio of local velocity to freestream velocity
u_p	Peak value of the velocity ratio
u_s	Separation value of the velocity ratio
V	Local velocity
V_∞	Freestream velocity
x	Distance from the nose along the chord divided by chord
x_s	Stagnation location
α	Angle of attack

LAMINAR SEPARATION

As discussed in Reference 2, the theory of Stratford, Reference 3, is very accurate. But, like most other methods it requires accurate, smooth longitudinal pressure gradients. Utilization of experimental pressures with attendant imprecision of measured pressures and pressure tap location proved impossible. Using the currently available powerful finite difference theories presented equal difficulties due to the inherent discontinuous pressure gradient.

A new method was derived based on that of Weber, Reference 4. While not mathematically rigorous, this method has proved to be of very high precision near the airfoil nose both in pressure level and in pressure gradient. It has been derived for the general airfoil shape, but is best illustrated for the uncambered airfoil. The local velocity is given by

$$\frac{V}{V_\infty} = u = \frac{A(x)\ \mathrm{Cos}\ \alpha \pm B(x)\ \mathrm{Sin}\ \alpha\sqrt{\frac{1-x}{x}}}{\frac{ds}{dx}}$$

The functions A(x) and B(x) are functions of the thickness distribution, but for most airfoils are nearly independent of x. Furthermore, the surface slope

function can be approximated by a parabola. Thus, the velocity and gradient are readily found by

$$u = \frac{A \cos \alpha \sqrt{x} + B \sin \alpha}{\sqrt{g + x}}$$

$$\frac{du}{ds} = \frac{1}{2}\left[\frac{A\, g \cos \alpha - (\pm B \sin \alpha)\sqrt{x}}{(x + g)^2} \right]$$

The stagnation (V = 0) location is therefore,

$$\frac{x_s}{g} = \left(\frac{B}{A}\right)^2 \frac{\tan^2 \alpha}{g}$$

It is convenient to give the local velocity in terms of the stagnation location, rather than angle of attack. It is apparent that the airfoil velocity distributions become universal functions of x/g and x_s/g as shown in Figure 1. It is also apparent that certain key events are also functions of these parameters as shown. In particular, the laminar separation point and conditions at that point are direct functions of x_s/g.

The Stratford method can be applied to the non-dimensional velocity distributions to derive a universal chart for the velocity, position, and gradient at separation. This is given in Figure 2. The figure can be used for any airfoil once the stagnation point is known. This formulation is particularly useful in that the correct non-dimensionalizing parameters become obvious.

BUBBLE BURST CORRELATION

The available two-dimensional airfoil data was analyzed using this method to determine boundary layer and velocity gradient parameters at the laminar separation point at or near the angle of attack for laminar bubble burst. The best correlation obtained is shown in Figure 3. The data scatter results from a $\pm$ 1/2 degree angle of attack precision in the bubble burst angle of attack data. It should be noted that velocity gradient parameter is a 1/7th power function of the Reynolds number parameter in keeping with the general postulation that bubble burst is a failure of the turbulence level to re-attach.

Figure 3 is a key element of airfoil analysis but is not the only factor. If the Reynolds number is high enough, transitions will occur prior to laminar separation, precluding bubble formation. There is no wind tunnel data available at high enough Reynolds number to demonstrate such a phenomenon. But, on the other hand, there is considerable data at very low Reynolds numbers to indicate what has been called long bubble stall. Presumably this occurs when the separated laminar boundary layer does not immediately transition to turbulent. It is therefore unable to re-attach and the so-called short bubble does not form. It is generally thought that this occurs for $R_\theta < 125$.

Post stall analyses are very difficult because of the total reliance on unreliable experimental pressure distributions. However, there is good evidence to lead to the conclusion that as the short laminar bubble bursts, the pressure distribution must adjust, with increasing angle of attack, so that conditions for laminar bubble burst are maintained. In other words, the bubble burst boundary applies not only for the burst angle of attack, but for post burst angles as well.

Figure 4 shows the sequence of events and the relation to two well known phenomena: leading edge stall, and thin airfoil stall. For instance, airfoil A is typical of moderately thin airfoils (i.e., 64A010). At very low angles of attack, laminar separation does not occur near the leading edge, but aft of maximum thickness (if at all). As angle of attack increases the separation moves to the airfoil nose and a short bubble forms. As angle of attack is increased up to the burst boundary, a typical short bubble is obtained with little impact on the overall forces and moments. Further increases in angle of attack cause a drastic reduction in lift as the laminar separation condition moves down the boundary.

In the case of airfoil B, typical of thinner airfoils (i.e., 64A006), the same sequence of events occurs. However as the bubble bursts, and as angle of attack is increased, conditions at laminar separation move below $R_\theta = 125$. The separated layer does not transist and the long bubble is formed. Lift continues to increase, but at a reduced rate.

MAXIMUM LIFT PREDICTION

While this research was aimed primarily at drag prediction at high angles of attack, it does form the basis for prediction of maximum lift for airfoils of the "leading edge stall" type. This is illustrated in Figure 5. The effects of a leading edge flap are shown on a 64A010 airfoil, and of a trailing edge flap on a NACA 0009 airfoil. In the former case, it was noted during the test that separation occurred at the hingeline for flap angles in excess of 15°. Up to this angle, the current method predicts both $C_{L_{max}}$ and angle of attack for $C_{L_{max}}$ very well.

In the case of the trailing edge flap, no attempt was made to adjust the predicted airfoil nose pressure distribution for viscous effects on the flap itself. Even so, the angle for $C_{L_{max}}$ is well predicted and the prediction for $C_{L_{max}}$ is consistent with the approximation.

CONCLUDING REMARKS

Rational approximation to airfoil theoretical pressure has yielded an accurate method for prediction of conditions at laminar separation and given insight into a universal correlation of the bubble burst phenomenon. This, in turn, has led to a basic understanding of thin airfoil and leading edge stall.

REFERENCES

1. Goradia, S. and Lyman, V., "Laminar Stall Prediction and Estimation of $C_{L_{max}}$," Journal of Aircraft, September 1974, Vol. II, No. 9.

2. Curle, N. and Davies, H.J. Modern Fluid Dynamics, Vol. I Incompressible Flow, The New University Mathematics Series 1968.

3. Stratford, B.S., "Flow in the Laminar Boundary Layer Near Separation," A.R.C. R&M 3002, 1957.

4. Weber, J., "The Calculation of the Pressure Distribution on the Surface of Thick Cambered Wings and The Design of Wings with a Given Pressure Distribution," A.R.C. R&M 3026, 1955.

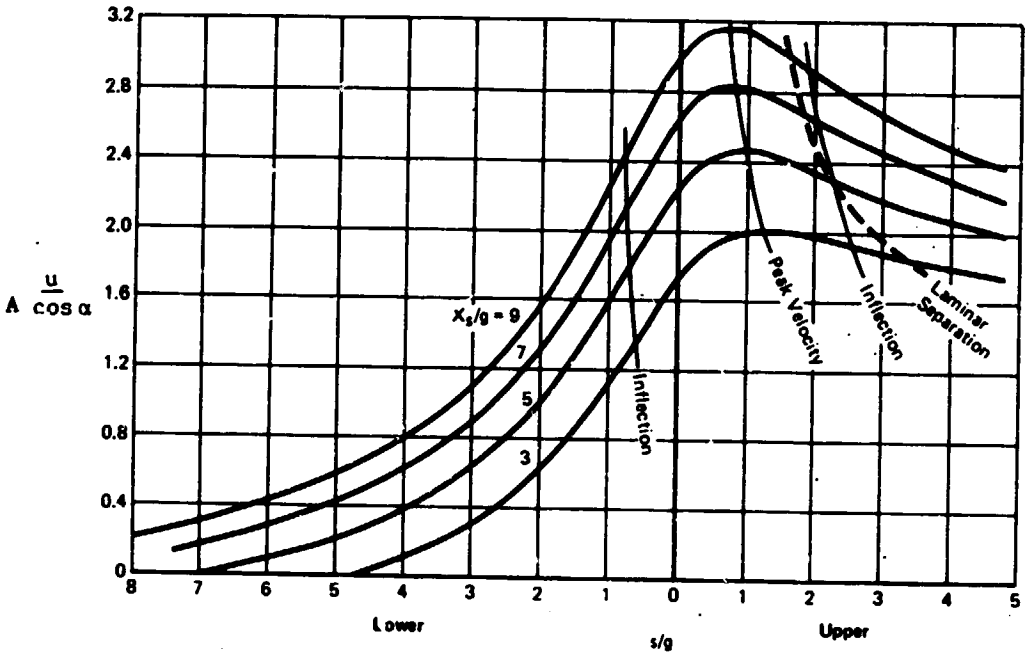

Figure 1.- Typical nondimensional velocity profiles.

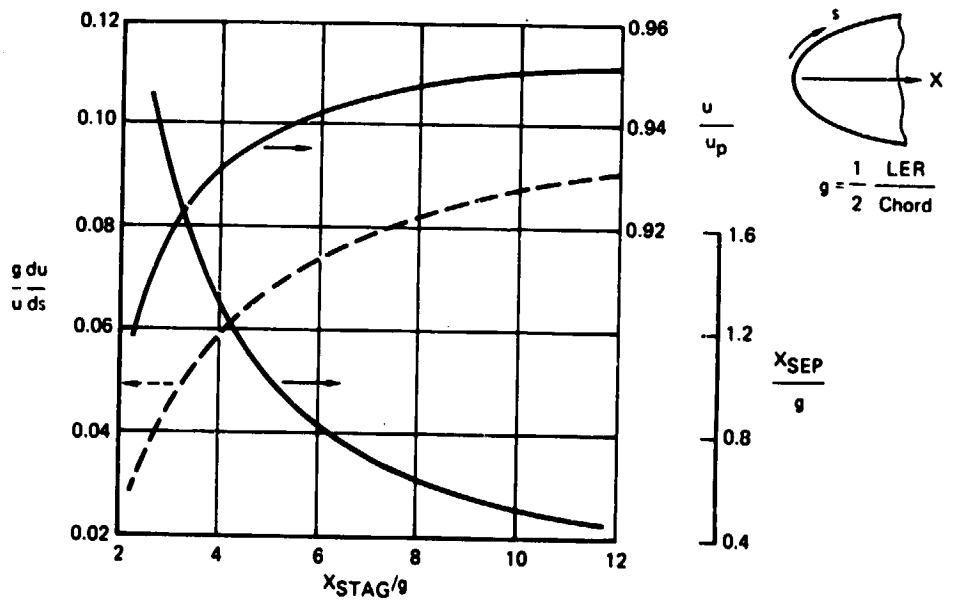

Figure 2.- Conditions at the laminar separation.

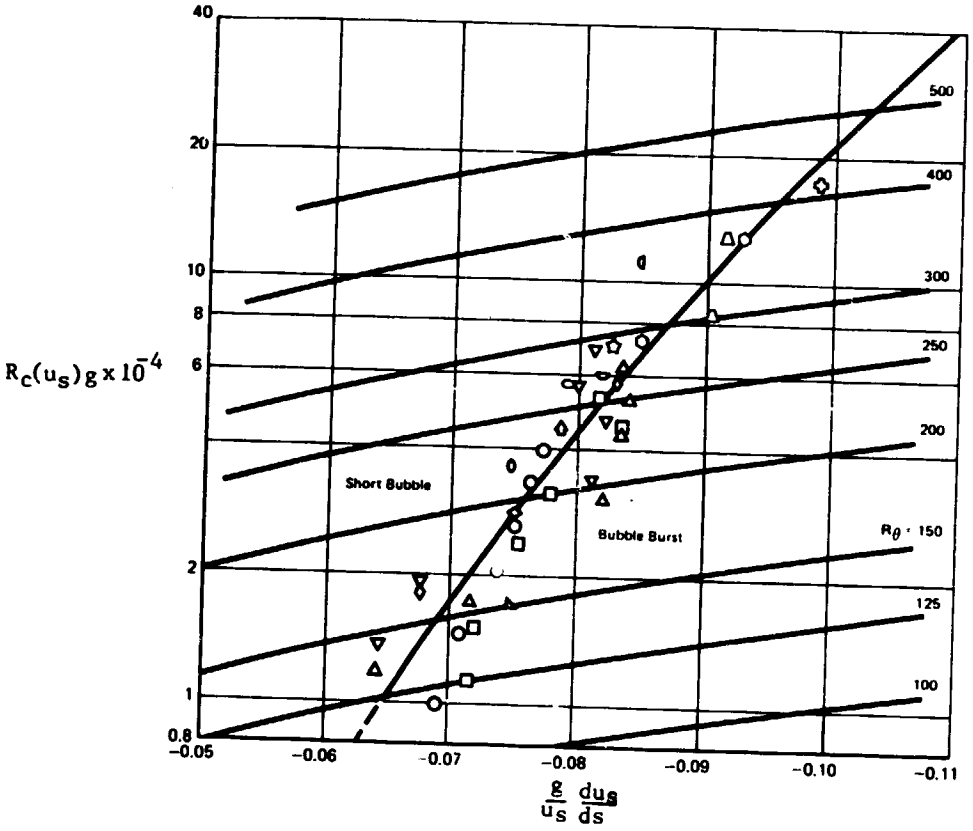

Figure 3.- Correlation of parameters affecting laminar bubble burst.

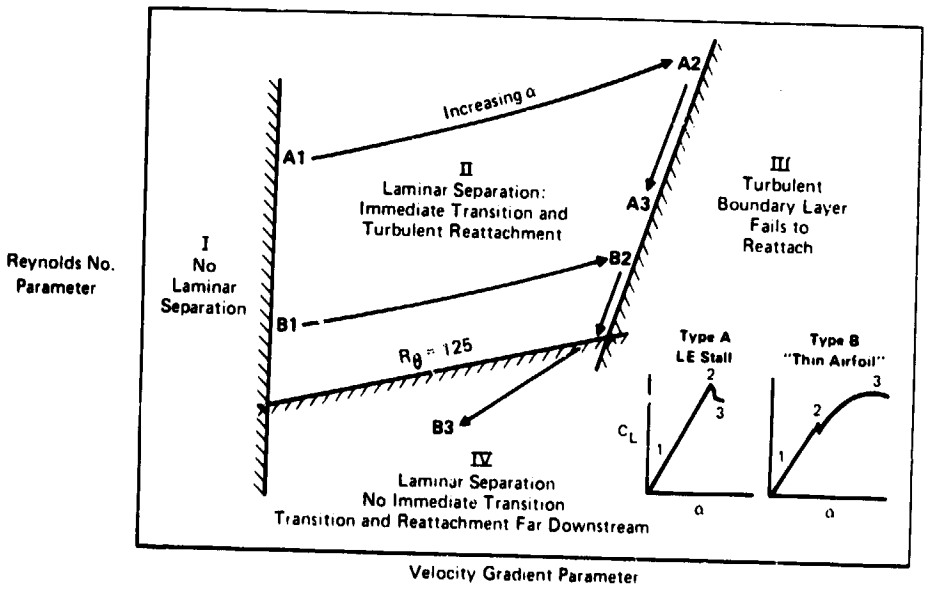

Figure 4.- Leading-edge stall development.

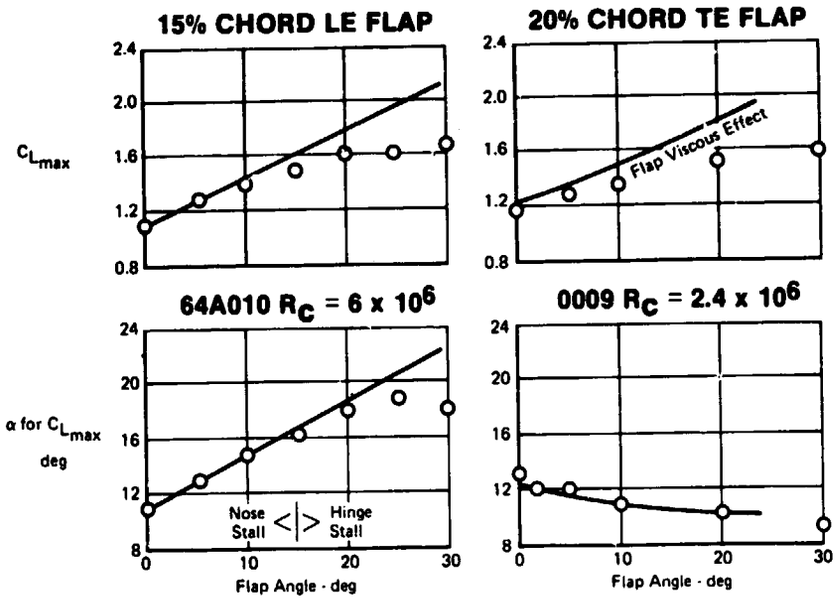

Figure 5.- Predicting leading-edge stall. Flapped airfoils.